U.P.B. Sci. Bull., Series D, Vol. 76, Iss. 3, 2014 ISSN 1454-2358

DESIGN PROCEDURE AND NUMERICAL ANALYSIS OF A SMALL HORIZONTAL-AXIS HYDROKINETIC TURBINE

Ion BADEA[1], Marius Gabriel COJOCARU[2], Mihai Victor PRICOP[3], Andreea BOBONEA[4]

The present work describes the initial design process of a horizontal-axis hydrokinetic turbine, using the blade element theory and an accurate CAD modeling. The results of such a process are presented and discussed for a small, 1kW turbine. The performance is then analyzed by means of CFD around the design point. The CFD results are obtained for different tip speed ratios and compared with the ideal curve.

Keywords: horizontal-axis hydrokinetic turbine, CFD, tip speed ratio, power coefficient, blade element theory.

1. Introduction

The kinetic energy of the marine currents is one of the renewable energies sources that have not been harvested yet. The usage of this type of energy has been studied in countries like Italy, France, Norway, Japan, USA, etc. and in the near future the interest in exploiting this resource is forecast to increase as the European community countries strive to achieve de goal of producing 20% clean renewable energy by the year of 2020.

Tidal stream are a specific part of the marine currents that present the most interest having speeds up to 4 m/s in near shore relative low depth locations. The worldwide potential of tidal streams is estimated at around 90-120GW and according to [1], the European potential is estimated at 15GW from which 60% is concentrated in United Kingdom's region as visible in fig. 1.

In this paper we present and evaluate by means of computational fluid dynamics an alternative for harvesting the tidal streams, marine currents and even river streams by using hydrokinetic turbines.

[1] MSc., Power Engineering Faculty, Hydraulics and Hydraulic Machinery Department, University POLITEHNICA of Bucharest, Romania, e-mail: ion.badea.07@gmail.com
[2] Eng., National Institute for Aerospace Research "Elie Carafoli"-INCAS, Bucharest, Romania
[3] Eng., National Institute for Aerospace Research "Elie Carafoli"-INCAS, Bucharest, Romania
[4] Eng., National Institute for Aerospace Research "Elie Carafoli"-INCAS, Bucharest, Romania

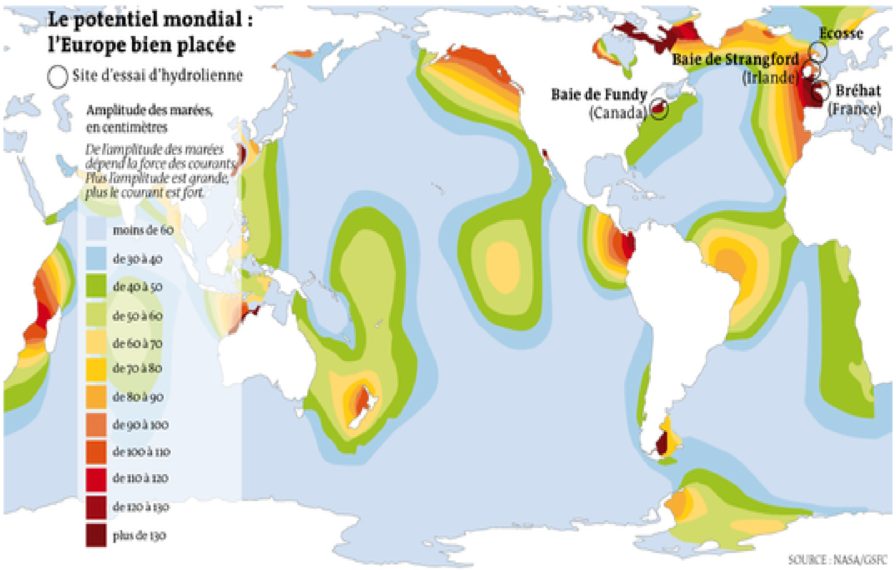

Fig. 1. The world's tidal streams potential map [Courtesy of NASA/GSPC]

For river applications the hydrokinetic turbines can be used mainly to extract the hydraulic energy of low head sectors of rivers that cannot be equipped with classical hydraulic turbines, such as Kaplan turbine, for economic reasons, but the potential of this resource has not been evaluated yet.

2. The turbine description and the design procedure

The turbine presented in this paper is a horizontal-axis hydrokinetic turbine used to extract the energy from marine/river currents with little environmental impact, by converting the kinetic energy of flowing water directly to mechanical power, without interrupting the natural flow [2].

The turbine has been dimensioned using the blade element theory, as implemented in [3] that was implemented into a MathCAD calculus sheet. Some modifications of the original routine have been done, in order to capture Reynolds dependency of the aerodynamic coefficients, together with a combination of different airfoils along the radius.

For this method we used as design input:

- the speed of the current, $V_{\infty} = 1.5$ m/s;
- the tip speed ratio, $\lambda = 2.5$;
- the number of blades, $z = 3$;
- the estimated power coefficient, lower than the Betz limit, $c_p = 0.375$;
- the amount of hydraulic power desired to be obtained, $P = 1$ kW.

A single NACA 4418 airfoil was chosen for which lift and drag coefficients have been computed, for different angles of attack, using the XFOIL tool. The angle of attack at the design point is set to vary from 9° at the tip of the blade to 12° at the root of the blade as recommended in Dumitrescu et al. [4].

The sizing of the rotor resulted in a diameter of 1.5 m which was determined using the kinetic turbine power equation:

$$D = \left(P \cdot \left(\frac{\pi}{4} \cdot c_p \cdot \frac{\rho}{2} \cdot V_{\inf}{}^3 \right)^{-1} \right)^{0.5} \tag{1}$$

In order to optimize the blade geometry a certain angle distribution for the relative velocity inclination was used:

$$\phi(r,\lambda) = (c_1 + k(c_2 + k(c_3 + k(c_4 + k(c_5 + kc_6)))))\frac{\pi}{180}, \tag{2}$$

where $c = \begin{pmatrix} 57.51 & -35.56 & 10.61 & -1.586 & 0.114 & -0.00313 \end{pmatrix}$ and $k(r,\lambda) = \lambda r$

The axial and tangential induced velocities, which vary radially, are further computed in order to determine the torque and power coefficients.

$$a(r,\lambda) = \frac{X(r,\lambda) - Y(r,\lambda)}{1 - X(r,\lambda)},\ a'(r,\lambda) = \frac{a(r,\lambda)}{Y(r,\lambda)},\ \varepsilon(r,\lambda) = a\tan\left(\frac{c_D(\alpha(r,\lambda))}{c_L(\alpha(r,\lambda))} \right), \tag{3}$$

where X and Y are simplifying notations for:

$$X(r,\lambda) = \frac{1}{\tan(\phi(r,\lambda) - \varepsilon(r,\lambda)) \cdot \tan(\phi(r,\lambda))},\ Y(r,\lambda) = \frac{k(r,\lambda)}{\tan(\phi(r,\lambda) - \varepsilon(r,\lambda))}. \tag{4}$$

In this algorithm a profile resistance parameter $\varepsilon(r,\lambda)$ was considered which is a function of drag and lift coefficients for different angles of attack along the radius.

From the rotor disc theory as shown in Burton et al. [5] the power coefficient of the turbine can be determined as a function of induced velocities, relative radius and tip speed ratio. In order to obtain de overall power coefficient for a given λ it is necessary to integrate this function along the relative radius:

$$c_p(\lambda) = 8\lambda^2 \cdot \int_0^1 r^3 \cdot a'(r,\lambda) \cdot (1 - a(r,\lambda))dr \tag{5}$$

The local solidity σ, having the tip speed ratio as a driving parameter, was used to compute the chord distribution, where z is the number of blades:

$$C(r,\lambda) = \frac{2\pi \cdot r \cdot \sigma(r,\lambda)}{z}, \tag{6}$$

$$\text{where } \sigma(r,\lambda) = 4\frac{a(r,\lambda)}{1 - a(r,\lambda)} \cdot \frac{\cos(\varepsilon(r,\lambda)) \cdot \sin(\phi(r,\lambda))^2}{c_L(\alpha(r,\lambda)) \cdot \cos(\phi(r,\lambda) - \varepsilon(r,\lambda))}; \tag{7}$$

The twist angle distribution along the radius $\beta(r,\lambda)$ was determined from the blade velocities triangles equation:

$$\beta(r,\lambda) = \phi(r,\lambda) - \alpha(r,\lambda) \tag{8}$$

The main output of the design method presented above consisted of:

- power coefficient curve as a function of tip speed ratio;
- chord distribution along the radius, fig. 2. left hand side;
- twist angle distribution along the radius, fig. 2. right hand side;

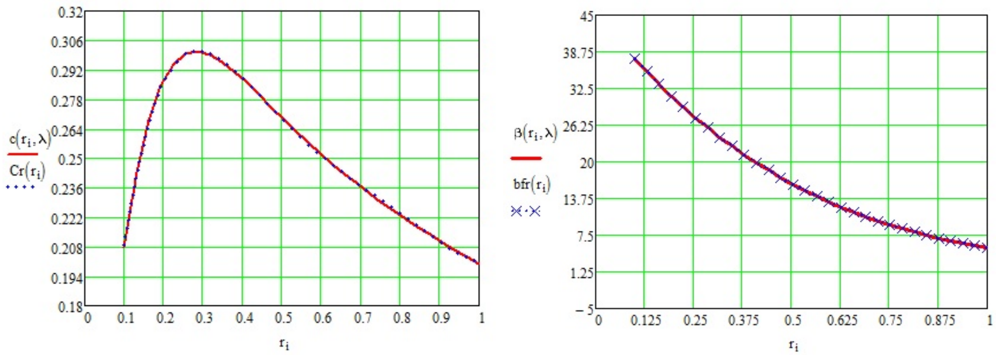

Fig. 2. Chord distribution (left), twist angle distribution (right)

As it can be noticed from fig.2, the chord varied from 0.26R at the root of the blade to 0.3R at 0.28 of radius and 0.2R at the tip of the blade, were R is the rotor's radius, while the twist angle varied from 34° at the root of the blade to 4.7° at the tip of the blade. In the design process the hub diameter has been considered to be equal to 15% of the rotor diameter.

The two curves, shown in fig. 2, have been approximated by a fifth degree, respectively a fourth degree polynomial function.

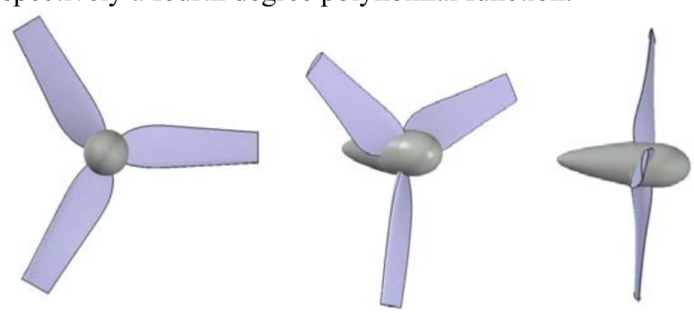

Fig. 3. The 3D geometry of the turbine in CATIA

The turbine geometry shown in fig.3 was generated in CATIA V5 using an in-house developed CATScript code (Visual Basic language), using analytical representations for airfoils, chord and twisting angle variations along the radius, as obtained from the blade element design routine. The least square, constrained polynomial functions of the chord and twist angle distributions, as well as the ones of the NACA4418 profile, were implemented as PARCurve elements, while the leading and trailing edge curves were introduced as combination of their analytical defined projections (3D Combine operator/API function).

3. Computational setup

The 3D numerical modeling of the viscous flow has been performed with the CFD commercial code FLUENT. The flow was assumed incompressible and fully turbulent. The shear-stress transport (SST) k-ω turbulence model developed by Menter [6] was used in order to combine the advantages of the robust and accurate formulation of the Wilcox k- ω model in the near-wall region with the free-stream independence of the k-ε model in the far field [7].

The simulations have been carried out using a finite volume discretization of the incompressible Reynolds averaged Navier-Stokes equations (RANS).

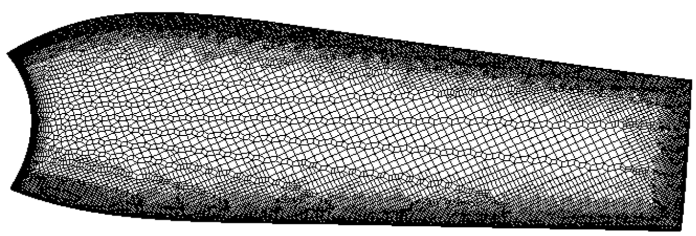

Fig. 4. The projected mesh on a blade

The mesh was generated in NUMECA's HEXPRESS tool, using hexahedral volume elements and consists of two domains, one considered stationary having over 0.3 million cells and another housing the turbine rotor having approximately 2.8 million cells.

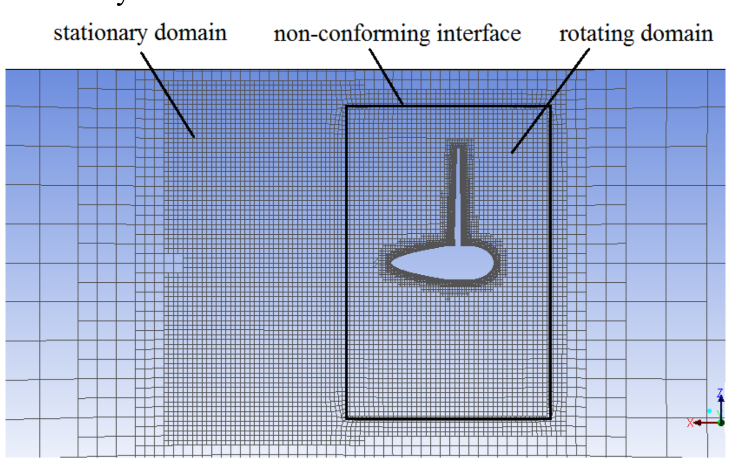

Fig. 5. The mesh in a longitudinal slice through the turbine

As the investigation was focused on the flow in the wake of the turbine and in the near-rotor domain, the mesh was refined in downstream and viscous layer inflation was used near rotor starting with a first layer height that enforces a y+ of 30, with a growing factor of 1.2.

The sizing of the two domains was similar to that suggested by Heinzelmann et al. [8]. The cylindrical stationary domain used the following dimensions 5R upstream, 13R downstream and 6.5R in radial direction, while the one of the moving reference frame domain, which includes the rotor, used a streamwise extension of 0.5R and 1.3R in radial direction.

The boundary conditions used were:

- At the Inlet the velocity-inlet boundary condition was preferred with a prescribed value of 1.5 m/s, speed that is common for some sectors of Prut river [9] and also for some sectors of Danube river [10];
- At the Outlet the 0 pressure outlet boundary;
- At the outer boundary of the stationary domain the slip wall boundary condition has been imposed;
- No slip wall condition for the blades and hub;
- In between the two domains non-conforming interface boundary conditions have been imposed.

For the first iterations a stationary case was considered with the purpose of obtaining the initial solution needed. Once the stationary solution converged, a multiple reference frame cell zone condition was considered as the method was found to be efficient in terms of computational time and resources.

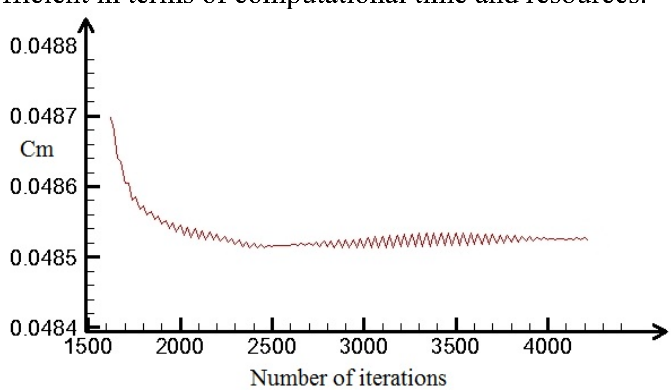

Fig. 6. The curve of the torque coefficient variation with the number of iteration

From the torque coefficient curve fig.6 it can be noticed that the computed solution for one of the cases analyzed stabilized after more than 4000 iterations around the value of 0.04854, corresponding to a power coefficient of 0.291.

4. Results

In order to illustrate the flow structure obtained from numerical simulations, the results were processed using Tecplot. Not only that this tool was found to be more intuitive than the post processing tool of ANSYS, but the resources needed to process the data were reduced about 8 times, from 3.2 GB of RAM up to approximately 550 MB of RAM while using a standard 4 GB of RAM laptop.

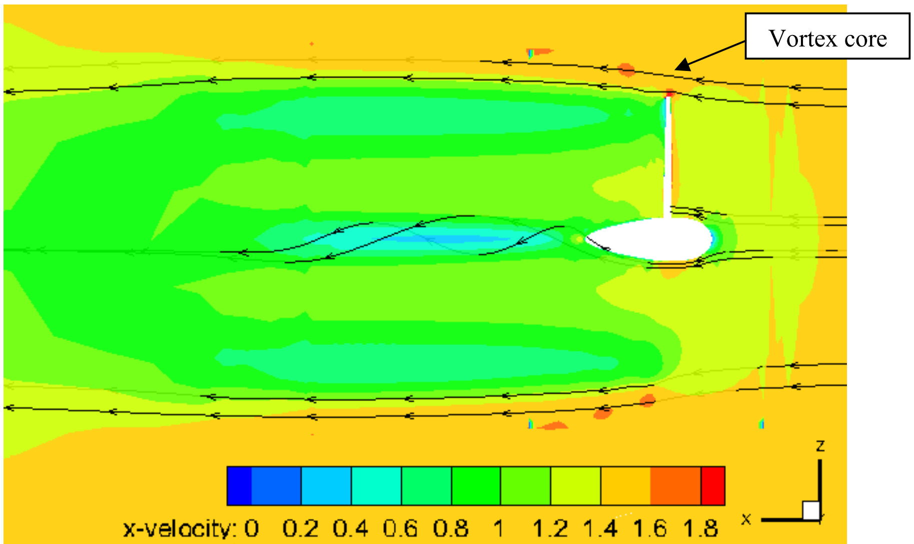

Fig. 7. Longitudinal velocity field

A longitudinal velocity field section is presented in fig.7 along with some representative streamlines. From this figure it can be noticed that the stream tube that enters the turbine rotor diminishes by a factor of 1.18 in diameter while the speed of the current entering the turbine decreases because of the blockage phenomenon.

At the same time, one can observe that there are two types of vortices that are formed in the wake of the turbine:

- a low velocity string vortex is formed in the wake of the hub having speeds up to 0;
- a high velocity vortex detaches from the tip of the blades having a speed of approximately 1.6 m/s in the direction of the flow.

The vortex formed from the tip of the blades can also be represented using isosurfaces having the velocity of 1.6 m/s as in fig. 8.

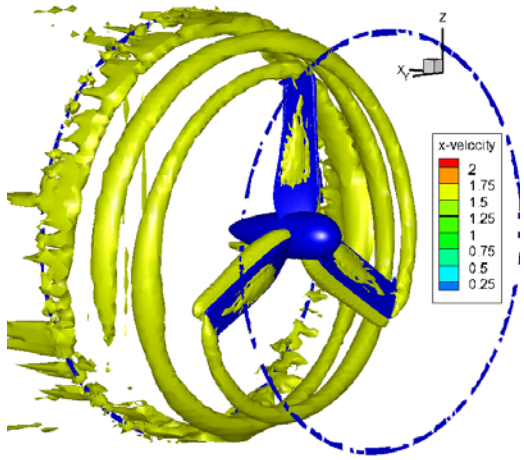

Fig. 8. The turbine vortex.

The high velocity vortex formed in the wake of the turbine is noticed to diverge after it separates from the blade tip, having a 25% larger diameter then the one of the turbine at a downstream distance of 0.4D.

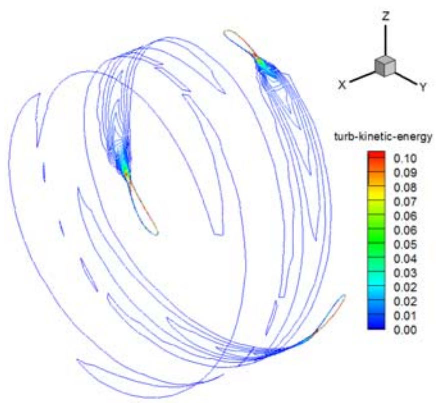

Fig. 9. The turbulent kinetic energy in a cylindrical section.

The turbulent kinetic energy for a cylindrical section placed at 0.5D is presented in fig.9. This representation is used to assess the velocity fluctuations responsible for noise produced by wind turbines [6].

The plot of the pressure distribution on the blades reveals that for an imposed tip speed ratio of 6 and for a rotor diameter of 1.5m the lowest relative pressure that can be found in around -0.5 bar. This means that the kinetic turbine designed in this paper functions in a non-cavitational regime even if it is submerged near the surface of the water. For greater diameter kinetic turbines being mounted on mobile platforms and functioning near surface, the critical point that can develop a cavitational regime is, as noticed in the right hand side plot in fig. 10, the leading edge of the tip of the blade.

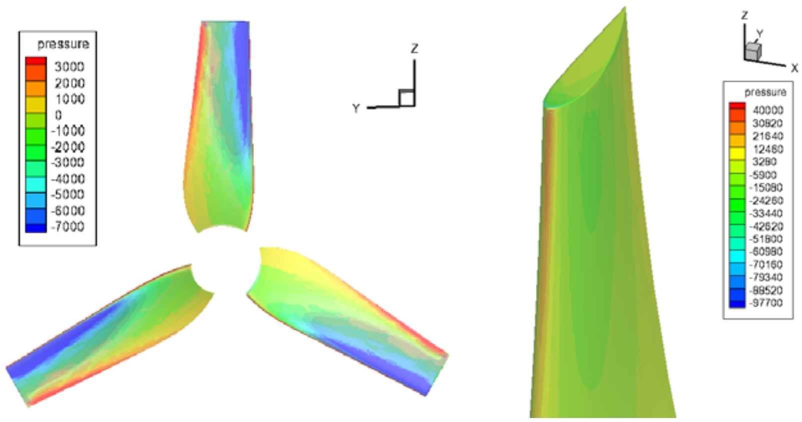

Fig. 10. Pressure distribution on the blades

An evaluation of the turbine performance was made by monitoring the torque used to determine the power of the turbine, respectively the power coefficient for different tip speed ratio:

$$P = M \cdot \omega \quad \Rightarrow \quad c_p = c_M \cdot \lambda \tag{9}$$

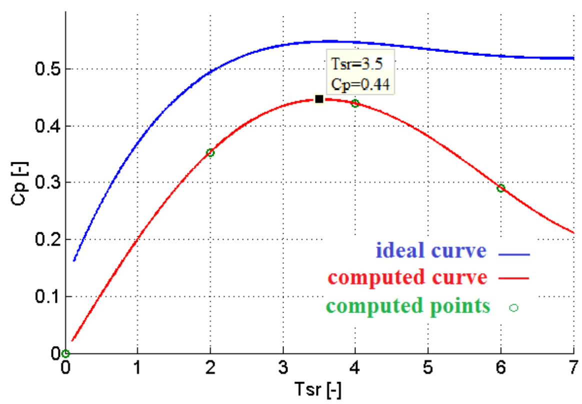

Fig. 10. The power coefficient curves of the turbine: cp=f(λ).

The ideal designed power coefficient curve and the computed power coefficient curve are shown in fig.10. One can observe that the optimal tip speed ratio takes the value of 3.5 while the optimal power coefficient exceeds the one used in the initial design having the value of 0.44.

6. Conclusions

The design procedure was proved to generate high power coefficient blade geometries having a power coefficient greater than 0.4 for tip speed ratios from

2.45 to 4.75. The numerical analysis was found to be useful for determining the peak functioning state of the turbine while the computed performance curve was found to present a root mean square deviation of 23% from the ideal designed performance curve.

For greater diameters it is recommended to shape the leading edge of the tip of the blade by rounding the tip or by using ailerons in order to avoid functioning in a cavitational state.

Further work will be dedicated to optimize the rotor's geometry by imposing as design tip speed ratio the one found to be optimal in this paper, having the value of 3.5, and making more numerical simulations near this working point.

Although the numerical analysis takes an important computing time, more numerical simulations at different velocities values are needed in order to design the gearbox and to increase the turbine global efficiency.

REFERENCES

[1]. *L. Dupin*, "Deuxieme round pour l'hydrolienne d'EDF", L'Usine Nouvelle, Brest, France, September, 2012

[2]. *A.-M. Georgescu*, *S.-C. Georgescu*, *A.-M. Petre*, *I. Badea*, "Time efficient computing of the power coefficient for a ducted Achard turbine", University "Politehnica" of Bucharest Scientific Bulletin, Series D: Mechanical Engineering (ISSN 1454-2358), **vol.74**, no. 4, pp. 189-200, 2012

[3]. *M. V. Pricop*, *M. L. Niculescu*, *M. G. Cojocaru*, *D. Barsan*, "Design, Analysis and Testing of Small, Affortable HAWT Rotors", Proceedings of AIP Conference, Kos, Greece, pp. 1646-1649, 2012

[4]. *H. Dumitrescu*, *A. Georgescu*, "Calculul elicei" (Blade design), editura Academiei Romane, Bucureşti, 1990.

[5]. *T. Burton*, *N. Jenkins*, *D. Sharpe*, *E. Bossanyi*, "Wind Energy Handbook, Second Edition", John Wiley & Sons, Ltd., Chichester, United Kingdom, 2011.

[6]. *FR. Menter*, "Zonal Two Equation k-ω Turbulence Models of Aerodynamic Flows", AIAA paper, 93-2906, 1993.

[7]. *M. L. Niculescu*, *M. D. Ionescu*, *M. Andrei*, *C. Cercel*, "Analysis of aerodynamic field and noise from a ducted wind turbine", Proceedings of the XXXIInd "Caius Iacob" National Conference on Fluid Mechanics and its Technical Applications, Bucharest, p.13, 2009.

[8]. *B. S. Heinzelmann*, *B. Gollnick*, *P. U. Thamsen*, *M. Petsche*, *J. B. Christiansen*, "Investigations into boundary layer fences in the hub area of wind turbine blades", European Wind Energy Conference, Brussels, p.10, 2008.

[9]. *I. Bostan*, "Sisteme de conversie a energiilor regenerabile" (Renewable energy conversion systems), Editura Tehnica-Info, Chisinău, 2007.

[10]. *C. Strechie-Sliwinski*, *L. Jugaru Tiron*, *S. Szobotka*, *R. Dimitriu*, *C. I. Pop*, "Viteze de curenţi şi debite ale apelor Dunării masurate cu ajutorul Sontek Riversurveyor ADP" (Current speeds and flow rates of Danube river measured with Sontek Riversurveyor ADP), in the preceedings of Ştiinţele Pământului, Cunoastere şi Mediu-Sesiunea anuală de comunicări ştiinţifice, GEO-ECO-MARINA, pp. 27-34, 2008.